Anal. Bioanal. Electrochem., Vol. 16, No. 6, 2024, 595-613
https://www.doi.org/10.22034/abec.2024.714093

Analytical & Bioanalytical Electrochemistry

2024 by CEE
www.abechem.com

Full Paper

Water Pollution Detection using CuO/Pre-Treated CTAB Modified Carbon Paste Electrodes: A Voltammetric Investigation

H.R. Dhrithi, and B.E. Kumara Swamy*

Dept of PG Studies and Research in Industrial Chemistry, Kuvempu University, Jnana Sahyadri, Shankaraghatta (577451) Shivamogga (D) Karnataka(S), India

*Corresponding Author, Tel.: +91-9900513796
E-Mail: kumaraswamy21@yahoo.com

Received: 25 April 2024 / Received in revised form: 15 June 2024 / Accepted: 16 June 2024 / Published online: 30 June 2024

Abstract- In the current effort, the nanoparticles of copper oxide (CuO/NP) were obtained by the co-precipitation procedure and characterized by the scanning electron microscope (SEM) X-ray powder diffraction (XRD), and energy dispersive spectroscopy (EDS) strategys. The CuO/MCPE was polymerized by utilising the N-Cetyl-N,N,N-trimethylammonium bromide (CTAB) surfactant, has been studied by cyclic voltammetric (CV) and linear sweep voltammetric (LSV) techniques. The analytical factors, such as pH, sweep rate, and concentration were evaluated. The limits of detection (LOD) and quantification (LOQ) was determined under optimized conditions and the values were arise to be 0.1179 µM, 0.391 µM, and 0.1942 µM, 0.6475 µM for Catechol (CC) and Hydroquinone (HQ), respectively. Moreover, the CuO/ pretreated CTAB/MCPE was employed for the sensitive and selective determination of CC and HQ in true samples.

Keywords- CuO nanoparticles; Catechol and Hydroquinone; Water pollutant; Voltammetry

1. INTRODUCTION

Although almost 70% of the Earth's surface is covered with water, just a limited portion (2.5%) of that is freshwater that could sustain lives on a terrestrial planet. Only about 40% of the water surface (transitional waters, coastal waters, rivers and streams,), and only 38% of them, are in good chemical health, according to a report from the European Environmental

Agency [1-2]. Industrialization, widened modern agricultural practices, and population-driven socioeconomic urban growth are all linked to environmental problems that lead to ruined water quality from pollutants like pesticides, nitroaromatics, bioaccumulative toxic heavy metal ions and phenolic substances like catechol (CC), and, hydroquinone (HQ) [3]. In the latter situation, several classes of contaminants might have accumulated over time through extended periods of unregulated garbage disposal, and replenishment might pose a significant technological issue [4]. Wastewater treatment frequently uses primary, secondary, or tertiary techniques depending on the type of pollutants**.**

The phenolic compounds, which include Catechol (1,2-dihydroxybenzene), Hydroquinone (1,4-dihydroxybenzene), and Resorcinol (1,3-dihydroxybenzene), are important isomers of dihydroxybenzene and are extensively utilized in the fields of antioxidants, agricultural substances, cosmetics, dyes and medicinal industries, etc. [5-9]. Due to their extensive distribution and diverse origins, isomers of dihydroxybenzene are significant environmental contaminants. They are harmful to people and challenging to disintegrate in natural environments [10]. Human sickness may develop from extremely low concentrations of CC and HQ. For instance, CC can result in malignant changes and mutagenesis [11-14]. The 1,2, and 1,4-dihydroxybenzene are important metabolites in the biological degradation of aromatic pollutants because of their water solubility, ease of microbial movement, and infiltration into the environment [15-19]. For the detection of dihydroxybenzene, a number of techniques have been used, including spectroscopy [20], chromatography [21], fluorimetry [22], voltammetry [23], high-performance liquid chromatography [24], trophotometry [25] and capillary electrophoresis [26–30]. Electrochemical techniques are attracting more interest than other techniques. It exhibits great sensitivity, quick reaction, low cost, ease of use, selective, consistent, powerful, and environmental friendliness [31–38]. An electrochemical approach, however, relies more on the concurrent identification of contaminants like HQ and CC because of their identical features and structural configuration, which allow anodic oxidation to take place practically at the same potentials [39-41].

Electropolymerization is a regularly used technology for the production of polymeric coating at the surface of bare electrodes. It has garnered significant attention from researchers for biosensor applications due to its potential electrocatalytic capability towards detecting of bio-active chemicals [42,43]. By optimizing the number of scanning intervals and the potential window, the analyst can manage the total thickness of the polymeric film through the implementation of this technology [44-46]. Carbon electrodes have been used in many well-designed surface modification applications because of their low cost and chemical inert qualities. Additionally, these devices have low electrical resistance and broad potential windows [47].

Nanoparticles are tiny particulates with a size between 1 and 100 nm and are gaining a lot of attention in a multiple of fields due to their peculiar physical and chemical attribute [48–51].

They are unique because of their ductility, electrical conductivity, and luminous efficiency. The brownish-black powder known as the copper oxide nanoparticles (CuO/NPs) has garnered a lot of curiosity. CuO/NPs is a p-type basic semiconductor with a tiny band gap, and it is a good choice because of its plentiful sources, little impact on the environment, cost-effectiveness, and use in agriculture, applications in biomedicine, and remediation of environmental damage. CuO/NPs are used to identify disorders and can be used to detect viruses in the human body [52-56].

Surfactants contain molecular structures assembled by themselves called as micelles in as solution, it has amphiphillic molecules with two functional groups. Due to amphiphillic molecules the interface between electrode and solution are altered at the electrode through adsorption. Because surfactants are inexpensive, easy to use experimental approach, and commercial availability, micelles are widely employed.

Adhesives present in carbon paste electrodes are hydrophobic in nature hence less substrate accumulates to the working electrode. The surfactants have the potential to improve this deposition process. N-Cetyl-N,N,N-trimethylammonium bromide (CTAB), Scheme 1, is a cationic surfactant and creates a single coat on the surface of the electrode with a high concentration of positive charges oriented away from the electrode [57-62].

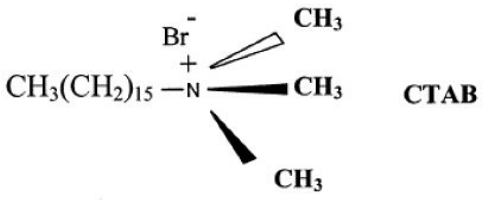

Scheme 1. Structure of CTAB

In the present study, the synthesized CuO/NPs were polymerized by CTAB and used as a fabricated carbon paste electrode for electrochemical analysis of CC and HQ with different parameters. The CuO/pretreated CTAB/MCPE exhibits excellent stability and repeatability, along with the real sample analysis.

2. EXPERIMENTAL SECTION

2.1. Chemicals and agents

The chemical substances mentioned are of analytical quality and were adopted without additional purification. Copper (II) sulphatepentahydrate ($CuSO_4.5H_2O$), Sodium hydroxide (NaOH), CTAB (N-Cetyl-N,N,N-trimethylammonium bromide), potassium ferrocyanide ($K_4Fe(CN)_6$), and potassium chloride (KCl) were purchased from Merk chemicals, Catechol (CC), hydroquinone (HQ), resorcinol (RS), and silicon oil were purchased from Himedia Mumbai, (India). Graphite powder was bought from Loba Mumbai, (India). The preparation of

buffer mixes involved combining $NaH_2PO_4.H_2O$ with $Na_2HPO_4.H_2O$ in different proportions, which were also obtained from Himedia. Double-distilled water was used to prepare all of the solutions.

2.2. Apparatus

Cyclic voltammetry (CV) and linear sweep voltammetry were achieved by the CHI-600D instrument. Three electrodes participated in this experiment, namely the working electrode, reference electrode, and auxiliary electrode. Bare and altered carbon paste electrodes were adopted as working electrodes, saturated calomel electrodes (SCE) were used as reference electrodes, and platinum wire was used as a counter electrode.

2.3. Synthesis of CuO nanoparticle

CuO/NPs were produced by facile co-precipitation process. 0.4 M copper sulphate was dissolved in a 100 ml of beaker containing 50 ml of distilled water and kept for stirring in a magnetic stirrer for about one hour, the prepared 1 M NaOH (in distilled water) solution was added to the beaker gradually until it reached pH 7.0. A brownish-black precipitation was obtained; the obtained precipitated solution was allowed to settle at ambient temperature and then filtered and efficiently cleaned with purified water and transferred to a hot air oven for further drying. The obtained particle was calcined at 400˚C for 4 hours in a muffle furnace [63].

2.4. Preparation of bare carbon paste electrode and modified carbon paste electrode

A bare carbon paste electrode (BCPE) was groomed by blending 70% graphite powder and 30% silicon oil for about 30 to 45 minutes to form a homogeneous mixture in an agate mortar. This paste is then loaded into a homemade Teflon cavity for further study.

To prepare a modified carbon paste electrode (MCPE), distinct amounts of synthesized CuO nanoparticles were adopted i.e., 2, 4, 6, mg of CuO nanoparticles were mixed with graphite powder and silicon oil for a homogeneous mixture and smoothed after filled into the cavity.

2.5. Pretreatment of CTAB on CuO/MCPE

In order to accelerate the surface area and peak current of copper oxide modified carbon paste electrode (CuO/MCPE), a 25 mM solution of CTAB was adopted and the potential was retained between 0.3 to 0.7V at the sweep rate of 100 mV/s with 5 consecutive cycles. The voltammogram gradually declined with an increased potential cycle during multiple cycles. This indicates that the CTAB was deposited on the surface of CuO/MCPE. After the

pretreatment, the MCPE was slightly dipped in the double distilled water for the removal of excessively adsorbed material and used for further investigation.

3. RESULTS AND DISCUSSION

3.1. Characterisation of CuO nanoparticle

X-ray diffraction powder was utilized for figure out the crystallinity and purity of synthesized nanoparticles. In 2Θ degree, there were diffraction peaks that were rather sharp and correlated to the crystal face of CuO/NPs. The JCDPS card number 801268 precisely matched and validated the peak area and intensity difference of the nanoparticles [64]. The size of the CuO crystal was estimated by Scherer's equation (1) and the mean size obtained was 17.9 nm (Figure 1).

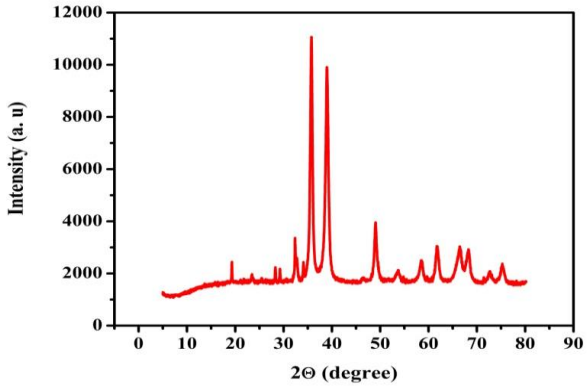

Figure 1. X-ray powder diffraction pattern for prepared nanoparticles

$$D = \frac{K\lambda}{\beta \, Cos \, \Theta} \text{ .....(1)}$$

Where K stands for constant (K = 0.94), λ for wavelength i.e. λ = 0.1543 nm, β for whole breadth half maximum intensity, and θ for diffraction angle of the diffraction peak under consideration.

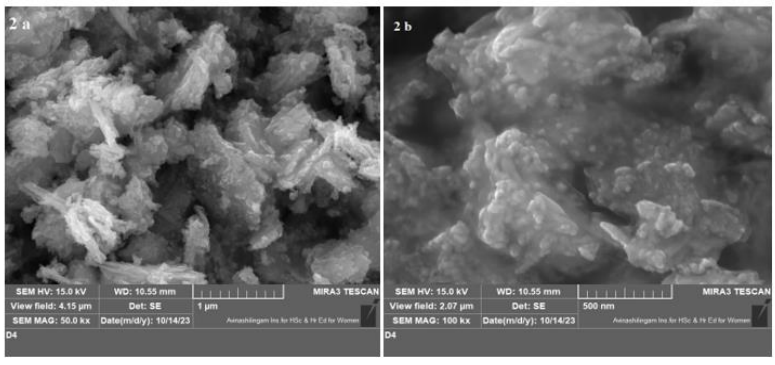

Figure 2. FESEM images for obtained CuO nanoparticle

To determine the nanoparticle's geometrical surface, FESEM examination was performed. Figure 2 demonstrates that the obtained CuO nanoparticles exhibit a multicrystalline structure and are easily distinguishable.

Figure 3. EDAX image for confirmation of copper and oxygen elements present in the synthesized nanoparticles

The effective production of the nanoparticle is demonstrated by the EDAX result, which unambiguously demonstrates that the generated nanomaterial is composed of Cu. The presence of carbon, oxygen, and copper in Figure 3 indicates that the particle was a CuO nanoparticle.

3.2. Optimal condition for working electrode:

In this study, the cycles were changed between five to twenty cycles. As the cycle increases (5 to 20 cycles) the current gradually decreases as shown in Figure 4(a) in 100mV/s scan rate. This represents the layer of surfactant formed exteriorly. The current reached its maximum in 5 cycles. Hence, 5 repetitive cycles were considered to study further parameters (Figure 4b).

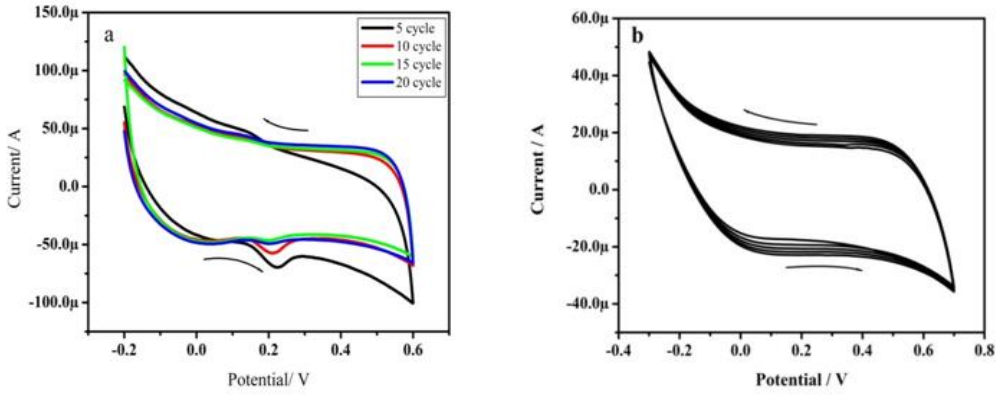

Figure 4. a) CV obtained from comparison of different cycles (5 to 20 cycles) at 100 mV/s; b) Pretreatment of CTAB on the surface of CuO/MCPE at 5 multiple cycles at scan rate 100 mV/s

As the working electrode was coated with CTAB, the area increased and the rate of electron transfer decreased due to meagre disclosure to a reactive site on the CuO/pretreated CTAB/MCPE. The thickness of the electrode was composed by developing the number of cyclic voltammetry parameters.

3.3. Comparative study for different amounts of CuO/MCPE

Through CV peculiar amounts i.e. 2, 4, and 6 of CuO nanoparticles were analysed in 1M KCl and 25mM $K_2[Fe(CN)_6].3H_2O$ with a sweep rate of 50 mV/s. Milligrams of CuO/NPs in different amounts are mixed with graphite powder and silicon oil. These homogeneous mixtures are kept in vowels for comparison study. The reduction and oxidation peaks are recognized in the voltammogram where the peak current inflation of 6 mg and deflation in 2, 4, mg was observed. 2.724e-5 A, 3.242e -5 A, 9.412e -5 A are the I_{pa} values of 2, 4, and 6 mg CuO/MCPE. As 6 mg shows a high peak current and it is preferred for further electrochemical analysis (Figure 5).

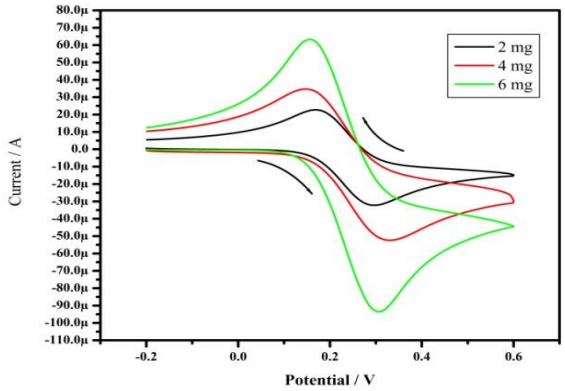

Figure 5. CV technique for comparison of 2, 4, 6 mg CuO nanoparticle at 1 M KCl and 25 mM $K_4[Fe(CN)_6].3H_2O$ at 50mV/s

3.4. Characterization of CuO/NPs pretreated CTAB/MCPE

Figure 6 indicates the characteristic properties of BCPE and CuO/NPs pretreated CTAB/MCPE accomplished in 1 M KCl and 25 mM $K_4[Fe(CN)_6].3H_2O$ at a scan rate 50 mV/s. The voltammogram displays a good enhancement in exterior area and redox peak current in MCPE in a study with BCPE. The ΔEp (discrepancy in redox peak potential) value of BCPE was noted to be 175 mV and 97 mV for MCPE, which indicates electron transfer and good electrocatalytic activity. The ΔE_p value is inversely proportional to the electron movement; the lower the ΔE_p value, the faster the electron transfer is achieved. A significant increase in the redox peak currents was noted at the modified carbon paste electrode (Figure 6) which represented the increase in surface area of the electrode. The total surface area can be calculated by Randles-Sevick's equation (equation 1).

$$I_p = 2.69 \times 10^5 \, n^{3/2} A D^{1/2} C_0 \, \nu^{1/2} \quad \ldots\ldots\ldots (1)$$

Where A is the electroactive surface area (cm^2), D is the diffusion coefficient (cm^2/s), ʊ is the scan rate (V/s), Co is the concentration of electroactive species (mol cm^{-3}), and Ip is the peak current (A). In comparison to BCPE, MCPE had a maximum electroactive surface area of 0.0433 cm^2 and 0.0246 cm^2 for BCPE.

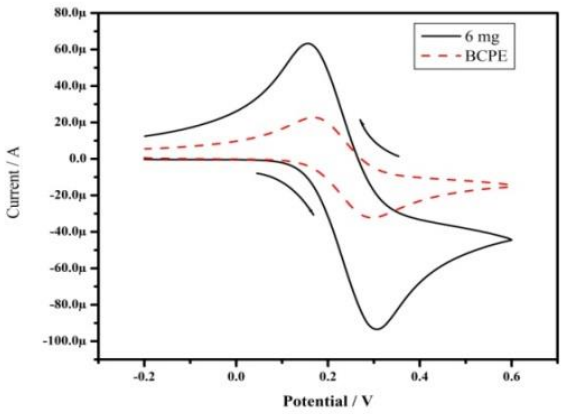

Figure 6. Dashed line represents BCPE and solid line represents CuO/ pretreated CTAB/MCPE by cyclic voltammetry technique at 50mV/s scan rate in 1 M KCl and 25mM $K_4[Fe(CN)_6].3H_2O$ solution

The CuO/NPs pretreated CTAB/MCPE displayed a higher peak current than the bare carbon paste electrode and the anodic peak current obtained with oxidation peak potential at 0.3061 V. Compared to other electrodes the CuO/NPs pretreated CTAB/MCPE showed higher sensitivity and increase the anodic peak current along with an increase in active surface area.

3.5. Comparison study with different surfactant

The surfactant was chosen after comparison with anionic (SDS), neutral (TX-100) and cationic surfactants (CTAB). In the presence of trace amounts of surfactants on the surface, the electrochemical response of CC at CuO/MCPE was inspected. The electrochemical reply of CC in the presence of surfactant was studied with 0.2M PBS of pH 7.4 at a sweep rate 100 mV/s. The peak current signal for BCPE was very weak in contrast with all three surfactants. CTAB shows enhancement in the area and an increase in peak current, whereas SDS and TX-100 does not show much difference compared to CTAB. Hence CTAB was used for pretreatment of the CuO/MCPE (Figure 7).

3.6. Electrocatalytic response of CC and HQ at CuO/ pretreated CTAB/MCPE

As cyclic voltammetry is a perceptive and authentic electroanalytical approach, electro-oxidation of CC was studied in this manner for both BCPE and MCPE. The electrochemical

cell containing 0.1 mM CC and 0.2 M phosphate buffer solution at pH 7.4 with a scan rate of 100 mVs^{-1} and the potential maintained between -0.2 to 0.6 V.

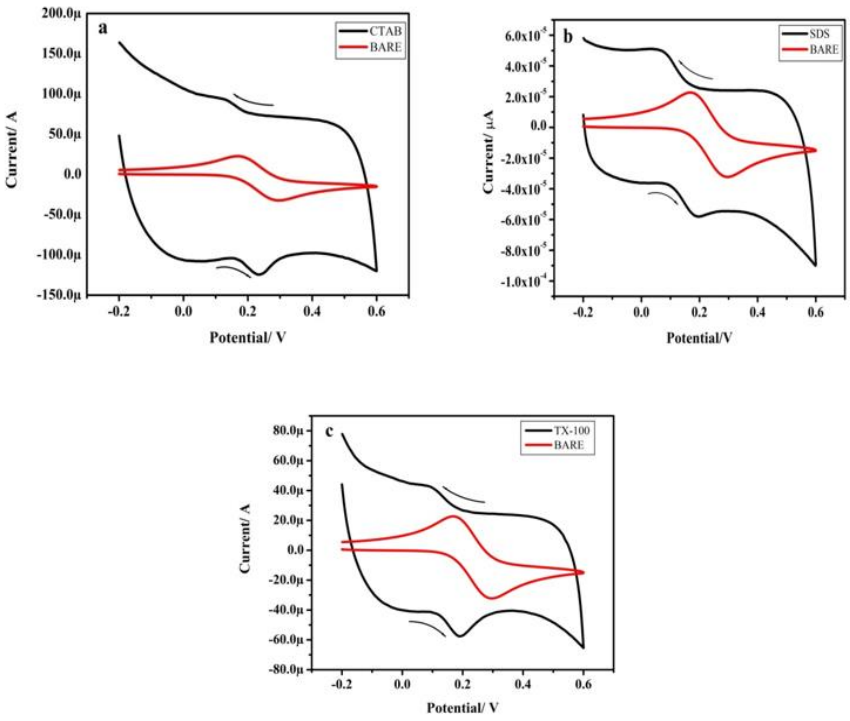

Figure 7. a) Comparison of BCPE with CTAB in scan rate 50mV/s; b) voltammogram of SDS and bare carbon paste electrode comparison; c) TX-100 surfactant using cyclic voltammetry with scan rate 50mV/s.

The current of the redox peak for CC at the unmodified carbon paste electrode responds less, and the altered carbon paste electrode exhibits good improvement. In CuO/ pretreated CTAB/MCPE negative shift in anodic potential is observed along with an increase in peak current.

For HQ the potential is controlled at -0.2 to 0.6 V, and the electrochemical cell contains PBS (0.2 M) solution (pH 7.4) and 25mM HQ. Comparing the modified electrode to BCPE, it exhibits better electrochemical performance. The oxidation at CuO/ pretreated CTAB/MCPE is influenced by the pH of the underlying electrolytes and exhibits changes in peak potential as well as current during the oxidation of HQ molecules. This shows that, during CC and HQ oxidation, protons -in addition to electrons are participated in and liberated from the CC and HQ molecules (Figure 8).

3.8. Influence of pH on CC and HQ at CuO/ pretreated CTAB/MCPE

For monitoring the CC at different pH ranges ranging from 6.6 to 7.8 was studied with the asses of CuO/ pretreated CTAB/MCPE. As the carrier electrolyte holds a major role in

recognizing the analytes, PBS was used as a carrier electrolyte with a scan rate at 100 mVs^{-1}. By increasing the pH, both anodic and cathodic peaks shifted toward positive and negative directions, and a comprehensible changeable redox of CC is seen in each pH solution. A stable oxidation peak can be seen in 6.6, 7, 7.8 pH, and a slight enhancement in peak current with pH 7.4 was observed. Hence, 0.2 M PBS of pH 7.4 was considered a working pH value for the upcoming analysis for CC. The portrayal indicates an increment in oxidation peak potential and a shift toward negative potential.

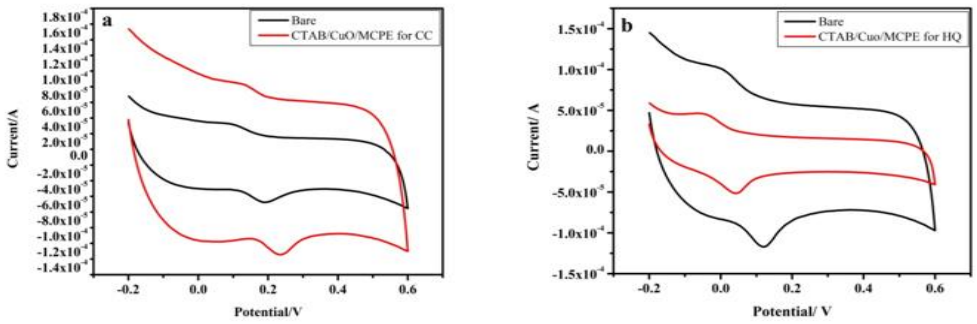

Figure 8. a) Cyclic voltammetry graph for 0.2 M PBS solution containing CC, black line indicating bare carbon paste electrode and red line indicating modified electrode; b) Voltammogram obtained for HQ in 0.2 M phosphate buffer solution, bare electrode signal was indicated by red line and the modified electrode was indicated by the black line.

pH 7.4 (0.2 M PBS) was acknowledged for the determination of other parameters in the existence of HQ, as it shows improvement in oxidation peak current compared to other pH values (6.2, 6.6, 7, 7.8) at the scan rate of 50 mVs^{-1}. The oxidation peak potential moves towards a negative way. As it is a pH-dependent process an equal number of electrons and protons were present in the chemical reaction (Figure 9).

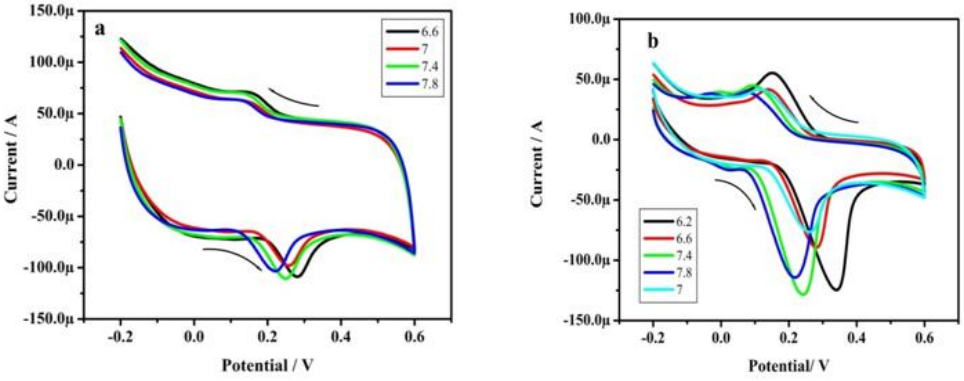

Figure 9. a)-Cyclical voltammetry for CC at CuO/ pretreated CTAB/MCPE achieved in the presence of various pH, b)-voltammogram represents various pH of HQ at CuO/ pretreated CTAB/MCPE

3.9. Effect of Scan rate

For the determination of the kinetics and transfer of electrons during the redox action of the stabbed analyte, a scan rate was carried out. The electrocatalytic activity of CC at CuO/ pretreated CTAB/MCPE for 50 to 500 mV/s in 0.2 M PBS at pH 7.4 was determined using the cyclic voltammetry technique. With an increase in scan rate, the peak current of isomers of dihydroxybenzene increases with excellent linearity. The I_{pa} (oxidation peak current) shifts to the positive side of the potential due to CuO/ pretreated CTAB/MCPE. Excellent linearity between I_{pa} and scan speed is demonstrated by the plotted curve (Figure 10b) and an acceptable correlation coefficient value $R^2 = 0.9952$ was obtained.

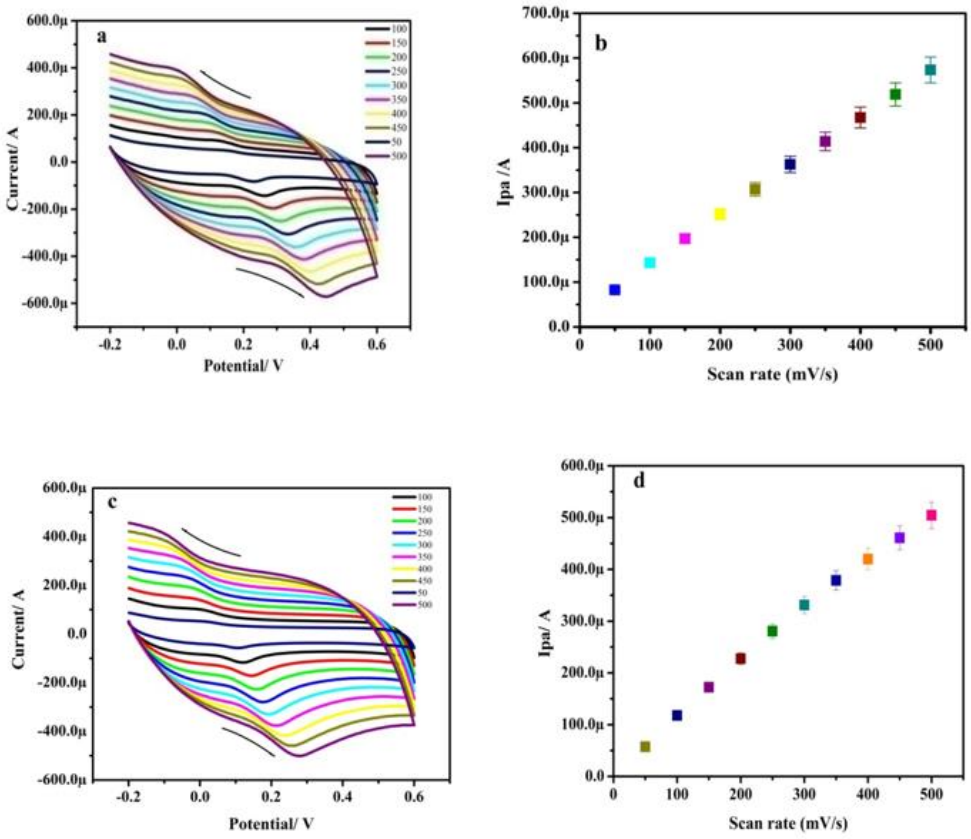

Figure 10. a) Cyclic voltammogram at CuO/ pretreated CTAB/MCPE with various scan rates, b) is the graph for potential v/s current at scan rate 50 to 500 mV/s, c) different scan rates for cyclic voltammetry of HQ at 50 to 500 mV/s, d) linearity graph of HQ at different scan rate

The electrocatalytic function of HQ was analysed by adopting CuO/ pretreated CTAB/MCPE at 50mV/s to 500mV/s scan rate in the presence of 7.4 pH (0.2 M PBS). The outcome shows that the I_{pa} and I_{pc} of HQ likewise increase with enhanced scan rate. Anodic and cathodic peak potential were increased and shifted towards the positive direction which expresses admirable linearity between scan rate and Ipa which can be observed in Figure 10(d). At high scan rate ΔEp i.e., peak-to-peak separation was insignificantly enhanced which is

illustrated in Figure 10(a) for CC and Figure 10(c) for HQ. The correlation coefficient value was found to be $R^2 = 0.9982$. This finding indicated the existence of an adsorption-controlled electrode mechanism (Scheme 2).

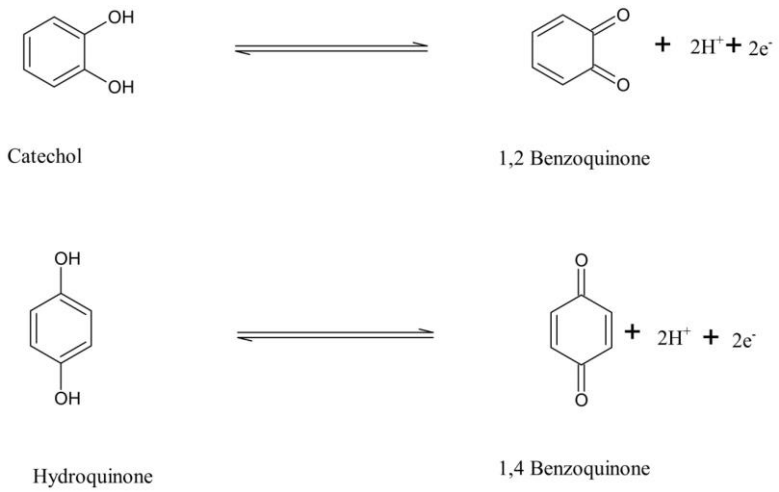

Scheme 2. Represents the mechanism of oxidation in CC and HQ

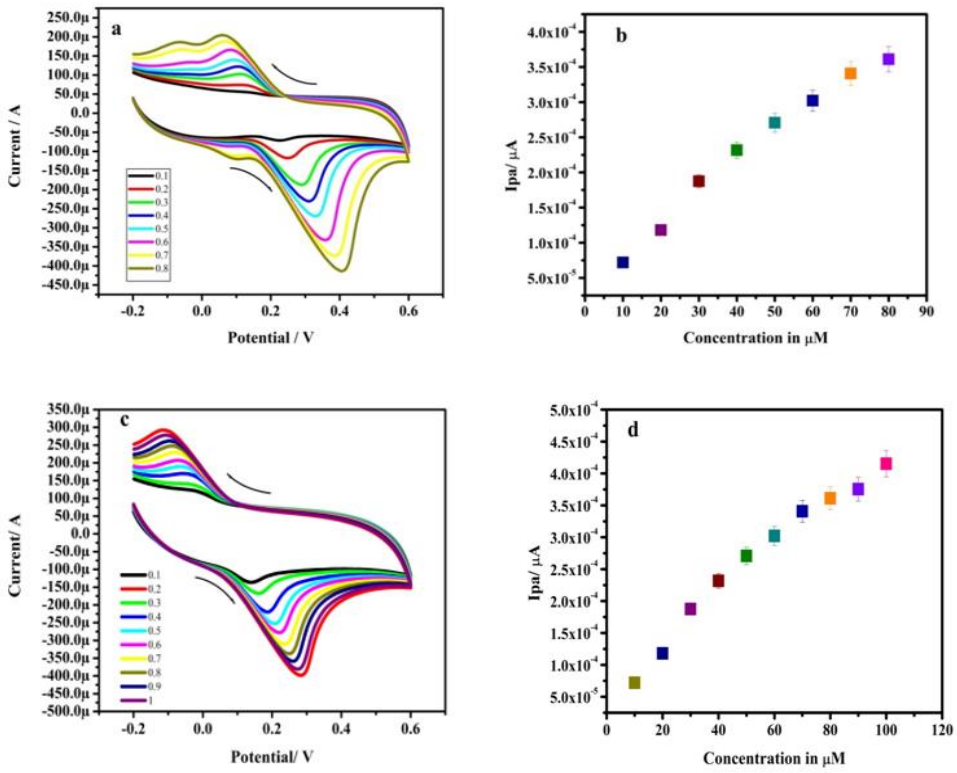

Figure 11. a) Study of CC concentration in the presence of CuO/ pretreated CTAB/MCPE, b) Voltammogram for linearity graph pH 7.4 and 0.2M PBS 100 mV/s, c) Concentration study of HQ at seep rate 50mV/s and 0.2 M PBS (pH 7.4), d) Linearity graph of HQ in 0.2 M PBS solution in 100 mV/s scan rate

3.9. Effect of concentration at CuO/ pretreated CTAB/MCPE

By increasing the concentration by 0.1 mM to 0.8 mM electrochemical oxidation of CC was analysed in the presence of working electrode CuO/ pretreated CTAB/MCPE with the sweep rate of 100 mVs^{-1}. Portray proved that anodic peak current (I_{pa}) increases by increasing the concentration and the peak potential (E_{pa}) and the current shifts to the positive direction for both CC (Figure 11a). Good linearity can be seen in the plot of I_{pa} vs CC concentration, R^2 = 0.9783 is the correlation value got form the graph (Figure 11b). The LOD was found to be 0.1179 µM and LOQ was determined to be 0.0324 µM.

HQ concentration was increased by 0.1 mM solution to 1 ml at a scan rate of 50 mV/s. As HQ rises, E_{pa} shifts somewhat in a positive direction while E_{pc} shifts in a negative direction (Figure 11c). It exhibits a great linearity and the correlation co-efficient value is R^2 = 0.9686. LOD and LOQ for HQ were found to be 0.1942 µM and 0.6475 µM respectively (Figure 11 d). For both CC and HQ, LOD and LOQ were calculated by adopting the formula 3S/M and 10S/M respectively. Where S represents deviation and M represents slope. Table 1 shows the comparison between CuO/pretreated CTAB/MCPE and other electrodes.

Table 1. Comparison of different electrodes with CuO/pretreated CTAB/MCPE

Sl. no.	**Working electrode**	**Technique**	**LOD(µM)**		**Reference**
			CC	**HQ**	
01.	PNR/MCPE	CV	6.46	4.97	[50]
02.	Poly(glycine)MCPE	CV	0.16	0.20	[51]
03.	LDHf/GCE	DPV	1.2	9.0	[52]
04.	MWNT/GC	DPV	0.2	0.75	[53]
05.	CNx/GCV	LSV	2.71	1.20	[54]
06.	RGO/MWNT	DPV	1.8	2.6	[55]
07.	CTAB/CUO/MCPE	CV	0.11	0.19	Present Work

3.10. Determining CC and HQ simultaneously with the existence of RS

The voltammetric response for isomers of dihydroxybenzene exhibits reduced selectivity and limited sensitivity due to its same phenolic structure and oxidation potential hence, it is difficult to detect the analyte in a mixture. Both CV (Figure 12a) and LSV (Figure 12b) technique was engaged for the electrochemical studies. The voltammogram indicates the coexistent studies of CC, HQ, and RS at a scan rate of 50 mV/s in 0.2 M PBS, pH 7.4. Compared to BCPE, CuO/ pretreated CTAB/MCPE shows distinguished peak potential. The

oxidation peak potentials of CC, HQ, and RS are located at 0.2315V, 0.1024V, and 0.5919V. Thus, it was considered an excellent sensor for the analysis of CC, HQ, and RS.

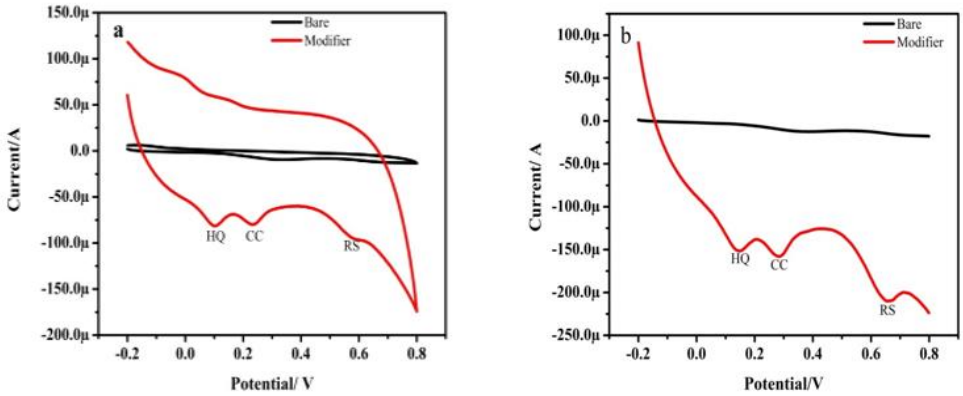

Figure 12. a) Cyclic voltammetry technique for simultaneous determination of CC, HQ, and RS at CuO/ pretreated CTAB/MCPE at 100mV/s and 0.2M PBS, b) Graph obtained from linear sweep voltammetry (LSV) for the detection of CC HQ and RS at 100 mV/s scan rate, pH 7.4

3.10.1. Interference test

For the study of selectivity and sensitivity of chosen analyte in a homogeneous mixture in the presence of CuO/ pretreated CTAB/MCPE by implying CV and LSV technique to ensure the clear discrimination of analyte. While HQ, RS are kept constant the amount of CC ranged from 0.1 to 1 mM in pH 7.4 (0.2 M PBS) with a scan rate of 50 mV/s and the voltammogram represents an increase in E_{pa} with a shift to a positive direction (Figure 13a). The same procedure was carried out while CC and RS concentrations were kept constant. RS is introduced to fine identification of peaks (Figure 13 b). Thus, proved that CuO/ pretreated CTAB/MCPE was reliable for the investigation of CC and HQ individually.

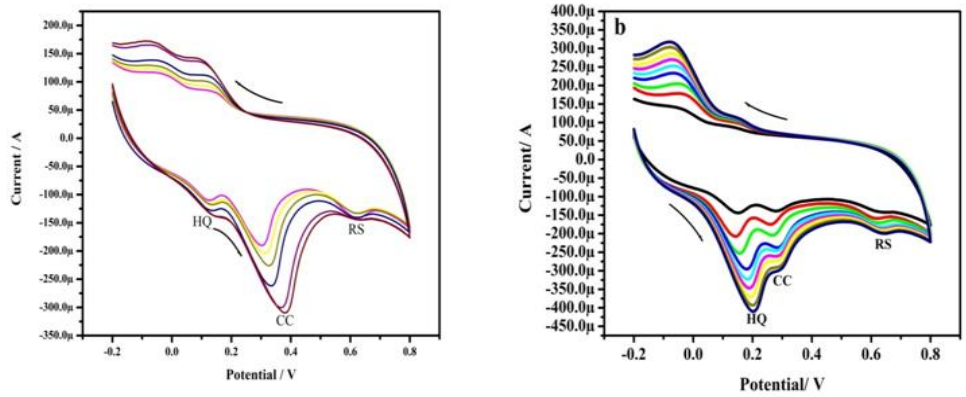

Figure 13. a) Interference study of CC while increase in concentration with pH 7.4 (0.2 M PBS) at scan rate 50mV/s where HQ and RS kept constant, b) Increased concentration of HQ where CC and RS were constant at universal pH, 50 mV/s scan rate

3.10.2. Stability and repeatability of CuO/ pretreated CTAB/MCPE

The stability of the CuO/pretreated CTAB/MCPE was evaluated in CC in pH 7.4 (0.2 M PBS) solution using cyclic voltammetry, with a sweep rate of 100 mV/s over 5 cycles.

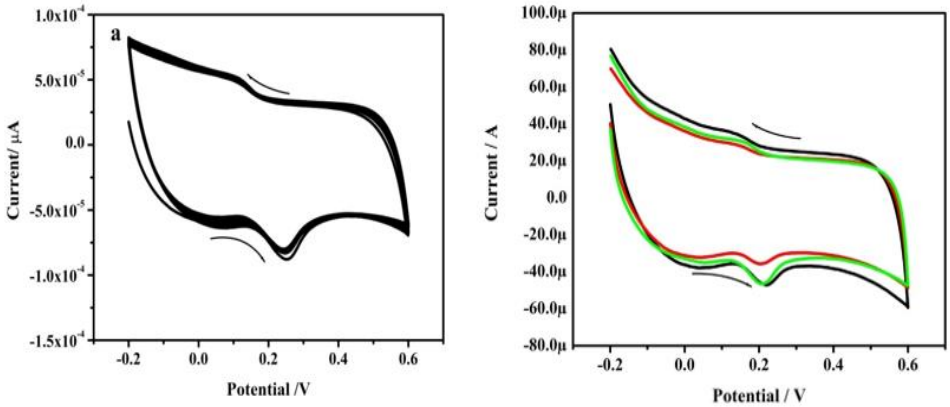

Figure 14. a) voltammogram for the stability of prepared CuO/ pretreated CTAB/MCPE by cyclic voltammetry method, b) Repeatability of CuO/ pretreated CTAB/MCPE by cyclic voltammetry technique at 0.2 M PBS (pH 7.4) at 100 mV/s

The redox potential is steady, and after completing 5 cycles, their oxidation peak current decreased. This demonstrates that the altered electrode is quite stable (Figure 14a). By monitoring the CV response of 0.1 mM CC in 0.2 M PBS solution (pH 7.4) at a scan rate of 100 mV/s within a potential range -0.2 to +0.6 V, the repeatability of the sensor is evaluated by CV and observed that the potential is almost stable in CC. Repeatability was assessed across three trials separated by two days (Figure 14b).

3.10.3. Analysis of real sample

The actual sample evaluation was performed using the addition process. i.e., by spiking a known amount of CC to squeezed tomato extract in order to validate the developed CuO/ pretreated CTAB/MCPE for the identification of CC in a true sample. The potential ranged from -0.2 to 0.6 at 100mV/s scan rate at pH 7.4. These findings unambiguously show that the sensor that was created may be successfully enforced for the disclosure of catechol levels in a real-life sample. Table 2 shows the obtained results.

Table 2. Detection of CC in real sample

Analyte	**Real sample**	**Added(µM)**	**Founded(µM)**	**Recovery (%)**
Catechol	Squeezed Tomato extract	10	9.178	91.780

4. CONCLUSION

CuO/ pretreated CTAB/MCPE sensor was designed to identify water pollutants like CC, and HQ by using both cyclic voltammetry and linear sweep voltammetry technique. CuO/ pretreated CTAB/MCPE exhibit strong electrocatalytic properties, high stability, sensitivity, and repeatability. The developed sensor displays a very minor limit of detection and quantification. A simple, low-cost, handleable, and quick time interval sensor was developed which is successfully justified for the disclosure of water contaminants like CC and HQ.

Declarations of interest

The authors declare no conflict of interest in this reported work.

REFERENCES

[1] J. Karpinska, and U. Kotowska, Removal of Organic Pollution in the Water Environment, Water 11 (2019) 2017.

[2] European Environment Agency, European Waters Assessment of Status and Pressures 2018; EEA: Copenhagen, Denmark (2018).

[3] C. Kumunda, A.S. Adekunle, B.B. Mamba, N.W. Hlongwa, and T.T.I. NKambule, Front. Mater. 7 (2020).

[4] K.I. Rajeshwar, J.G. Ibanez, and G.M. Swain, J. Applied Electrochem. 24 (1994) 1077.

[5] K. Chetankumar, B.E. Kumara Swamy, and S.C. Sharma, Mater. Chem. Phys. 252 (2020) 123231.

[6] H. Zhao, Y. Wang, S. Qian, C.F. Xu, W. Li, X. Li, D. Su, and Z. Hu, Int. J. Electrochem. Sci. 14 (2019) 1997.

[7] Y. Ma, Z. Cao, Y. Wang, Y. Xia, C. He, L. Wang, S. Bao, P. Yin, L. Wang, J. Gao, H. Wang, and Z. Yin, Int. J. Electrochem. Sci. 14 (2019) 3916.

[8] F. Tian, H. Li, M. Li, C. Li, Yi. Lei, and B. Yang, Synthetic Metals 226 (2017) 148.

[9] L. Hong-Ying. Z. Lang-Lang, H. Zhi-Heng, Q. Yu-Bing, X. an-Xiao, W. Jia-Jun, X. Wei-Wei, L. Li-Hua, and G. Chun-Chuan, Chinese J. Anal. Chem. 47 (2019) 19113.

[10] Y. Zhang, S. Xiaoa, J. Xie, Z. Yang, P. Pang, Y. Gao, Sens. Actuators B 204 (2014) 102.

[11] Y. Peng, Z.R. Tang, Y.P. Dong, G. Che, and Z.F. Xin, J. Electroanal. Chem. 816 (2018) 38.

[12] E.H. El-Ads, N.F. Atta, A. Galal, and N.A. Eid, Int. J. Electrochem. Sci. 13 (2018) 1452.

[13] X. Feng, W. Gao, S. Zhou, H. Shi, H. Huang, and W. Song, Anal. Chim. Acta 805 (2013) 36.

[14] Y. Xiang, L. Li, H. Liu, Z. Shi, Y. Tan, C. Wu, Y. Liu, J. Wang, and S. Zhang, Sens. Actuators B Chem. 267 (2018) 302.

[15] X. Cao, X. Lancai, Q. Feng, S. Jia, and N. Wang, Anal. Chim. Acta 752 (2012) 101.

[16] K. Chetankumara, B.E. Kumara Swamy, and S.C. Sharma, J. Electroanal. Chem. 849 (2019) 113365.
[17] Q. Chen, X. Lia, X. Min, D. Cheng, J. Zhoua, Y. Li, Z. Xie, P. Liu, W. Cai, and C. Zhang, J. Electroanal. Chem. 789 (2017) 114.
[18] D. Jiang, J. Pang, Q. You, T. Liu, Z. Chu, and W. Jin, Biosens. Bioelectron. 124–125 (2019) 260.
[19] Z. Liu, Y. Zhang, C. Bian, T. Xia, Y. Gao, X. Zhang, H. Wang, H. Ma, Y. Hu, and X. Wang, Biosens. Bioelectron. 126 (2019) 51.
[20] P. Nagaraja, R.A. Vasantha, and K.R. Sunitha, Talanta 55 (2001) 1039.
[21] W. Si, L. Wu, Y. Zhang, M. Xia, F. Wang, and Q. Hao, Electrochim. Acta 85 (2012) 295.
[22] P. Yang, Q. Zhu, Y. Chen, and F. Wang, J. Appl. Polym. Sci. 213 (2009) 2881.
[23] L. Jia, X. Zhang, Q. Li, and S. Wang, J. Anal. Chem. 62 (2007) 26.
[24] W. Si, L. Wu, Z. Han, Q. Hao, Y. Zhang, and M. Xia, Sens. Actuators B: Chem. 199 (2014) 154.
[25] P. Nagaraja, R.A. Vasantha, and K.R. Sunitha, J. Pharm. Biomed. Anal. 25 (2001) 417.
[26] S. Cogal, Anal. Lett. 51 (2018) 1666.
[27] P. Nagaraja, R.A. Vasantha, and K.R. Sunitha, Talanta 55 (2001) 1039.
[28] W. Si, W. Lei, Y. Zhang, M. Xia, F. Wang, and Q. Hao, Electrochim. Acta 85 (2012) 295.
[29] P. Yang, Q. Zhu, Y. Chen, and F. Wang, J. Appl. Polym. Sci. 2153 (2009) 2881.
[30] S. Cogal, Anal. Lett. 51 (2018) 1666.
[31] V.K. Gupta, H. Karimi-Maleh, and R. Sadegh, Int. J. Electrochem. Sci. 10 (2015) 303.
[32] K.V. Gupta, A.K. Singh, and L.K. Kumawat, Sens. Actuators B Chem. 195 (2014) 98.
[33] V.K. Gupta, N. Mergu, L.K. Kumawat, and A.K. Singh, Talanta 144 (2015) 80.
[34] M.L. Yola, V.K. Gupta, T. Eren, A. Emresen, and N. Atar, Electrochim. Acta 120 (2014) 204.
[35] V.K. Gupta, L.P. Singh, R. Singh, N. Upadhyay, S.P. Kaur, and B. Sethi, J. Mol. Liq. 174 (2012) 11.
[36] V.K. Gupta, M.R. Ganjali, P. Norouzi, H. Khani, A. Nayak, S. Agarwal, Crit. Rev. Anal. Chem. 41 (2011) 282.
[37] S.K. Srivastava, V.K. Gupta, and S. Jain, Anal. Chem. 68 (1996) 1272.
[38] N. Hareesha, and J.G. Manjunatha, Scientific Reports 11 (2021) 12797.
[39] V.K. Gupta, A. Nayak, S. Agarwal, and B. Singhal, Combinatorial Chem. High Throughput Screen. 14 (2011) 284.
[40] T.S.S. Kumar Naik, M.M. Mwaurah, and B.E. Kumara Swamy, J. Electroanal. Chem. 834 (2019) 71.
[41] S.S.K. Naik, and B.E. Kumara Swamy, J. Anal. Bioanal. Electrochem. 9 (2017) 424.

[42] J.G. Manjunatha, M. Deraman, N.H. Basri, and I.A. Talib, Arabian J. Chem. 11 (2018) 149.
[43] S. Staffan, A. Cheritat, J. Backstrom, and Ann Cornell, J. Electrochem. Sci. Eng. 7 (2017): 51-64.
[44] P.A. Pushpanjali, J.G. Manjunatha, B.M. Amrutha, and N. Hareesha, Materials Research Innovations 25 (2021) 412.
[45] P.A. Pushpanjali, J. G. Manjunatha, N. Hareesha, Edwin S. D'Souza, M.M. Charithra, and N S. Prinith, Surfaces and Interfaces 24 (2021) 101154.
[46] P.A. Pushpanjali, J.G. Manjunatha, G. Tigari and S. Fattepur, Anal. Bioanal. Electrochem. 12 (2020) 553.
[47] R. Chenthattil, J.G. Manjunatha, and G. Tigari, Instrumentation Sci. Technol. 48 (2020) 561.
[48] K.V. Harisha, B.E. Kumara Swamy, P.S. Ganesh, and H. Jayadevappa, J. Electroana. Chem. 832 (2019) 486.
[49] C.M. Kuskur, B.E. Kumara Swamy, and H. Jayadevappa, J. Electroana. Chem. 833 (2019) 512.
[50] K.G. Manjunatha, B.E. Kumara Swamy, H.D. Madhuchandra, and K.A. Vishnumurthy, Chemical Data Collections (2020) 100604.
[51] C.M. Kuskur, B.E. Kumara Swamy, and H. Jayadevappa, J. Electroana. Chem. 833 (2019) 512.
[52] M. Ahamed, H.A. Alhadlaq, M. Khan, P. Karuppiah, and N.A. Al-Dhabi, J. Nanomater. 5 (2014) 519.
[53] C.M. Panduranga, E. Niranjana, B.E. Kumara Swamy, B.S. Sherigara, and K.V. Pai, Int. J. Electrochem. Sci. 3 (2008) 588.
[54] J. Dong, X. Qu, L. Wang, C. Zhao, and J. Xu, Electroanalysis 20 (2008) 1981.
[55] F. Hu, S. Chen, C. Wang, R. Yuan, D. Yuan, and C. Wang, Anal. Chim. Acta 724 (2012) 40.
[56] K.S. Siddiqi, and A. Husen, Biomater. Res. 24 (2020) 1.
[57] R.P. Kumar, S. Senapati, A.K. Sahoo, I.M. Umlong, R.R. Devi, A.J. Thakur, and V. Veer, RSC Advances 4 (2014) 40580.
[58] M.S. Vishwanath, B.E. Kumara Swamy, and K.A. Vishnumurthy, Mater. Chem. Phys. 289 (2022) 126443.
[59] T.S.S. Naik, and B.E.K. Swamy, J. Electroanal. Chem. 804 (2017) 78.
[60] K.V. Harisha, B.E. Kumara Swamy, and E.E. Ebenso, J. Electroanal. Chem. 823 (2018) 730.
[61] M. Li, F. Ni, Y. Wang, S. Xu, D. Zhang, S. Chen, and L. Wang, Electroanalysis 21 (2009) 1521.
[62] H.Q.C. Zhang, Electroanalysis 17 (2005) 832.

[63] S. Reddy, B.E. Kumara Swamy, and H. Jayadevappa, Electrochim. Acta 61 (2012) 78.
[64] J.G. Manjunatha, Chemical Data Collections 25 (2020) 100331.